Sensors and Materials, Vol. 11, No. 8 (1999) 493–505
MYU Tokyo

S & M 0391

Capacitive SiO Humidity Sensors with Novel Microstructures

Andy T. Wu, Mary Seto and Michael J. Brett

Department of Electrical and Computer Engineering, University of Alberta,
Edmonton, AB, Canada, T6G 2G7

(Received June 7, 1999; accepted August 24, 1999)

Key words: sensor, new sensing material, new sensor fabrication technique, humidity sensor, SiO film, glancing angle deposition

It is demonstrated that porous SiO films fabricated by a newly developed glancing angle deposition (GLAD) technique can be used for relative humidity (RH) sensing. The sensing characteristics of capacitive SiO sensors depend critically on the details of their microstructures. It is shown that a SiO sensor with a microstructure of cylindrical rods and a porosity of 25% can exhibit a response time of less than three seconds for a stepwise change in RH from 15% to 80%. The sensor does not degrade after water immersion and has a dynamic response range over five orders of magnitude. The conventional equivalent circuit model is shown to be inadequate in explaining the observed results. It is suggested that the detailed microstructure of the entire sensor and the interactions between water moisture, the SiO film and the applied field must be taken into consideration in calculating the total parallel capacitance of the SiO sensor when RH reaches a certain level. Our results indicate that the GLAD technique has broad potential in various sensing applications, due to the ease of fabrication of porous films with structure controllable in three dimensions on the 10 nm scale.

1. Introduction

Relative humidity (RH) sensing is an important process required in many areas, for example, precision instruments, semiconductor chip manufacturing, food and chemical processing industries, automobile industry, and environmental chambers, as well as air conditioners. Among different types of sensors[1] used for RH sensing, the capacitive type has been playing an important role because it can be fabricated cheaply in different sizes and can be incorporated relatively easily into integrated circuits. Nowadays, two types of capacitive RH sensors are commonly used and investigated: polymer and ceramic. Capacitive polymer RH sensors usually have good linearity in their working range. Hysteresis as small as 0.5% RH is achievable in the sensing range from 10 to 90% RH when an appropriate polymer is chosen as the sensing material.[2] Typical response time is about four minutes,[3] which can be improved considerably by using an obliquely deposited metal electrode.[4] Due to the inherent water-reactive nature of most polymers, intensive exposure to high RH or water immersion can degrade or even destroy polymer sensors. The dynamic response range of polymer sensors is narrow, typically[3] from 110 to 144 pf for a change of RH from 8% to 90%. Ceramic capacitive RH sensors usually have a wider dynamic response range and do not react with liquid water. A dynamic response range of four orders of magnitude has been recorded.[5] On the other hand, linearity is not as good and they often exhibit a relatively large hysteresis loop.[6] Although RH sensing has been used and investigated since the invention of the first hygroscope by Nicolas Cryfts in 1450, humidity measurement remains a difficult task for the design engineer,[7] and research and development are being actively pursued.

Recently, a new film deposition technique for porous film fabrication, called glancing angle deposition (GLAD), has been developed[8] at the University of Alberta. By combining oblique angle evaporation with controlled substrate motion, this technique allows us to fabricate films with three-dimensional control of the structure on the 10 nm scale. Possible optical applications of this technique have been demonstrated,[9,10] and potential applications in biological, mechanical, magnetic, and electrical fields[11] have been suggested. In this paper, we demonstrate that this technique can be used for sensing applications. Capacitive humidity sensors are fabricated using SiO films, deposited by the GLAD technique, as the sensing material. It is shown that the sensors have fast response times, a wide dynamic response range, and do not degrade after water immersion. Initial experiments show two advantages of these sensors: the sensing characteristics of the sensors can be finely tuned to different sensing needs by tailoring their microstructures, and a wide range of dielectric substances may be used as the sensing material. The latter point is further supported by the recent advance in the GLAD technique. It has been shown that in addition to thermal and e-beam evaporation methods,[8] GLAD-fabricated films can also be grown by sputtering[12] and laser ablation[13] methods, thus enabling the deposition of metals, semiconductors, dielectric materials, organic materials, and refractory materials. Here, we use RH sensing only as an example to illustrate the utility of the GLAD technique in sensing applications. Based on this example, we suggest that the GLAD technique can be used to produce films for many other sensing applications where a large surface/mass ratio is desired or a particular microstructure is required.

2. Experimental

There are several reasons why we have chosen SiO as the RH sensing material. First, it is well known that SiO is relatively chemically inert and does not react with liquid water. Therefore, the sensors are less likely to degrade after water immersion or after long-term use under conditions of high humidity. Also of importance is the fact that the dielectric properties of SiO films are relatively well studied, and SiO films may be readily fabricated using thermal or e-beam evaporation, to which the GLAD technique is commonly applied.

The basic principle of the GLAD technique is schematically illustrated in Fig. 1. The substrate is rotated about two axes. One is perpendicular to the substrate plane (ϕ rotation), the other parallel (α tilt). A computer is used to control the ϕ rotation and α tilt. Different combinations of the speed and the direction of the ϕ rotation and the tilting angle of the substrate allow us to fabricate films with various microstructures. Film porosity is determined primarily by α, with increasing porosity for increasing α. Various microstructures, for instance, helices, "zigzags", "staircases", or posts, can be produced by the GLAD process with porosity controllable from 10 to 80%. A detailed description of the GLAD process and achievable microstructures is given in ref. 8.

The layout of our SiO RH sensor is shown in Fig. 2. Aluminum electrodes were first deposited onto an insulating substrate. Then the GLAD technique was used to thermally evaporate porous SiO films with different microstructures surmounted by denser capping layers. The vapor source material we used was random pieces of SiO. Typical dimension of the SiO pieces was from 3 to 6 mm and purity was 99.9%. Deposition conditions were

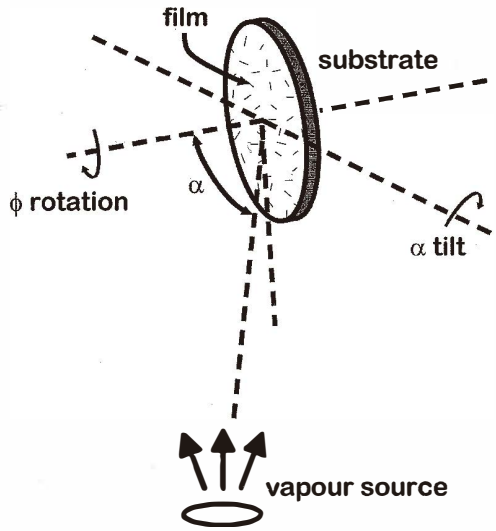

Fig. 1. The basic principle of the GLAD technique.

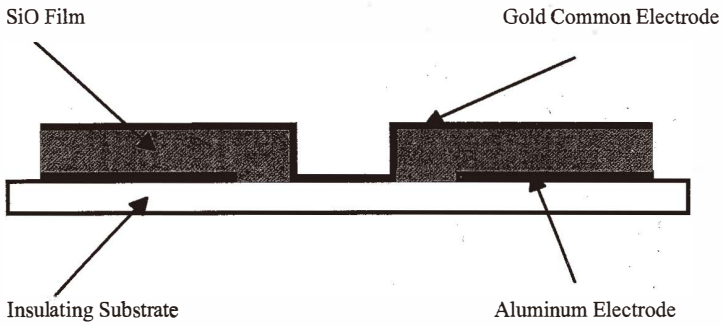

Fig. 2. Schematic layout of our SiO RH sensor.

kept fairly constant, with typical deposition rates of 20~30 Å/s and base pressures of 3.5×10^{-6} Torr. Energy-dispersive X-ray diffraction (EDX) measurements indicated that the obtained films were mainly SiO. Finally, a gold layer was sputter deposited on top of the capped SiO as a common electrode. In this report, we will focus our attention on two representative examples of SiO sensors with post and helix microstructures.

Capacitance-RH (C-RH) curves were measured using the control system shown in Fig. 3. This system allowed RH to be varied between 1% and 97%. When a RH below room humidity was desired, we put desiccants into the container inside the humidity chamber. For high RH, water was placed into the container instead. A switch was used to change the electronic circuit from one state to the opposite when RH was varied from below room humidity to above room humidity or vice versa. During the change, we needed to put a dish of either water or desiccants behind the outer fan. The electronic circuit was essentially a proportional-integral-differential control loop. It compared the output of the standard RH sensor with the value set by a potentiostat, and produced a pulse width modulation to the fan driver according to the magnitude of the difference between the output of the standard RH sensor and the set value. The internal fan was used to accelerate the evaporation of liquid water or the absorption of moisture by desiccants inside the humidity chamber and to make the environment in the humidity chamber more homogeneous. Dry or wet air was blown into the humidity chamber employing the outer fan. The dry or wet air was then mixed with the air inside the humidity chamber to produce a particular RH. The sample was placed as close to the standard RH sensor as possible. A commercial capacitance meter was used to measure the parallel capacitance of the sample at 120 Hz.

Measurements of the response to a step change of RH were carried out by putting the sample into a sealed dish at room humidity inside the humidity chamber. The RH of the chamber was increased to 80%, and the cover of the sealed dish was removed. The time required for the capacitance of the sample to increase to 90% of its capacitance at 80% RH was measured as the response time. Since the seal might not be completely tight, we took a small amount of leakage into account by viewing the step change of RH as being from 15% to 80%. All measurements were carried out at 23°C.

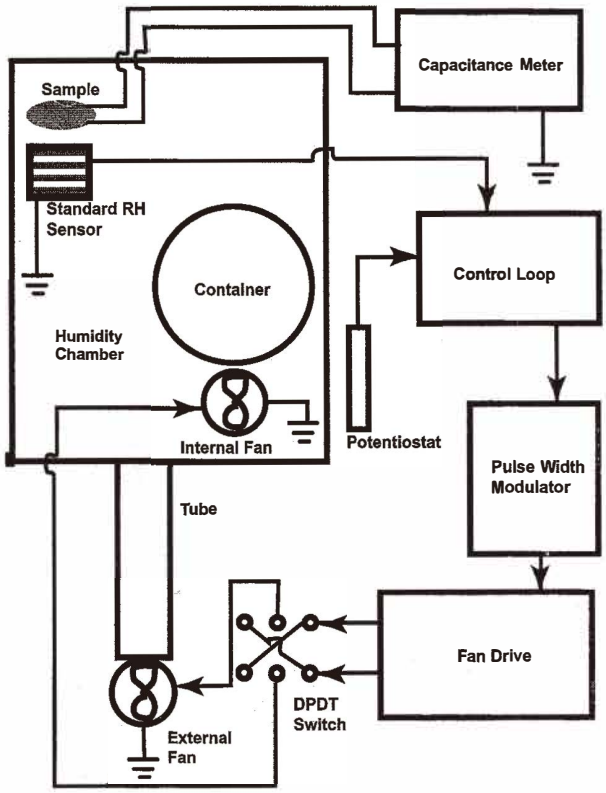

Fig. 3. Schematic block diagram of our measuring system.

3. Results and Discussion

A scanning electron microscope (SEM) cross-sectional image of one of our sensors is shown in Fig. 4. The SiO capacitor layer was grown by choosing an appropriate tilting angle α with substrate rotation to produce a porous film with helical microstructure. A more compact layer of SiO film (called a capping layer) was then deposited on top of the helical SiO film by exponentially decreasing the tilting angle α while lincarly increasing the speed of the substrate rotation ϕ. Finally, a gold layer was sputter deposited on top of the capping layer with a thickness varying from sensor to sensor, depending on the detailed microstructure of the capping layer and desired gold film porosity. For the sensor (Sensor A) shown in Fig. 4, the thickness of the gold layer was estimated to be around 30 nm. The thicker appearance of the gold layer in Fig. 4 is an artifact created by the high ductility of Au during cleaving and sample preparation. This thin gold layer contained natural perforations due to grain boundaries and islanding, which formed passages through which

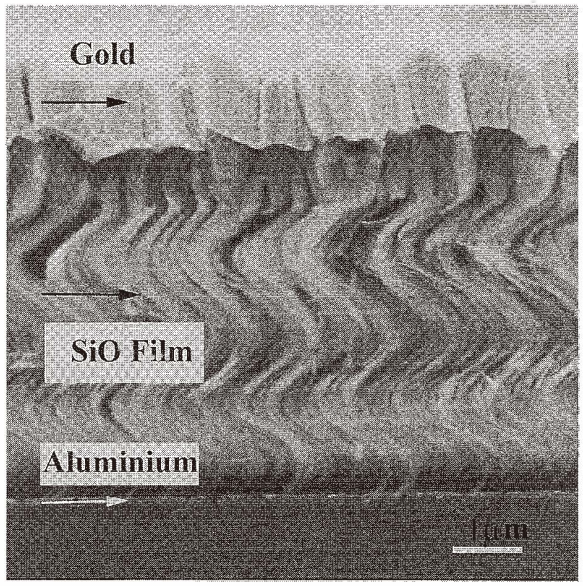

Fig. 4. SEM cross-sectional image of Sensor A.

water molecules can move freely in or out of the interior of the sensor. The capacitance of this sensor was measured as a function of RH at room temperature (see Fig. 5). The observed capacitance first increased slowly and linearly with RH up to about 85% RH where a sharp increase in sensitivity occurred. With decreasing RH, hysteresis developed down to 60% RH.

3.1 *Effect of microstructure of SiO film*

The importance of the microstructures of the sensing materials to the characteristics of the sensors was clearly demonstrated in the work by Shimizu and coworkers.[14,15] Their results indicated that pore size distribution in ceramic humidity sensors had a decisive influence on the sensing characteristics of the sensors. To study this effect, we prepared Sensor B with a different microstructure, as shown in Fig. 6. The fabrication procedure of this sensor is similar to that of Sensor A except that the tilting angle α is larger and the speed of substrate rotation ϕ is much faster. The relatively more compact layer near the substrate is caused by the fact that during nucleation and initial bulk growth stages, the self-shadowing effect is less prominent. The corresponding C-RH curve is shown in Fig. 5. A dramatic change in the shape of the curve, the hysteresis loop, and the dynamic response range is observed. The hysteresis loop of Sensor B is present over a much wider RH range than that of Sensor A. Most surprisingly, the dynamic response range of Sensor B covers five orders of magnitude in capacitance. This wide dynamic response range was common

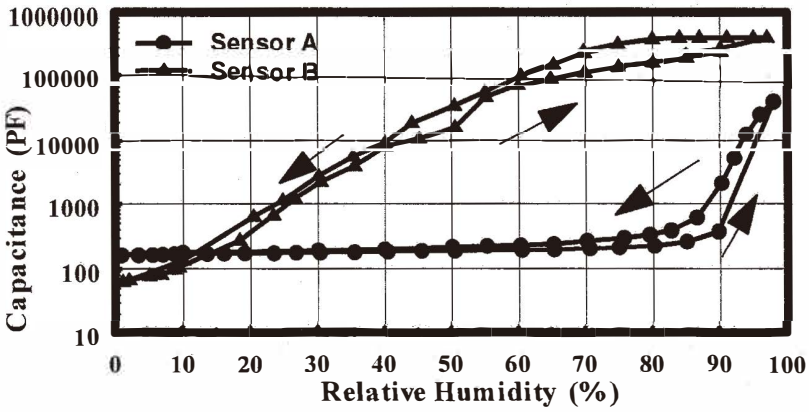

Fig. 5. Capacitance versus relative humidity for Sensors A and B. Arrows indicate the direction of RH cycling.

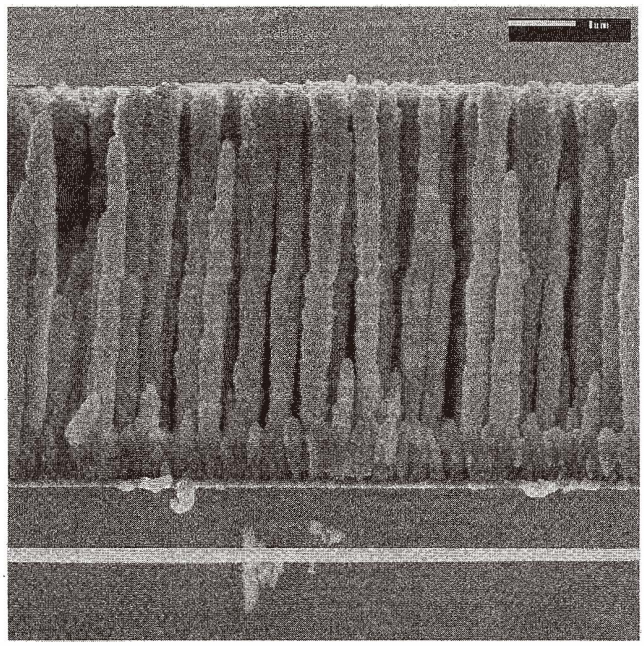

Fig. 6. The microstructure of Sensor B.

to a number of sensors fabricated with similar post microstructures. Other researchers have recorded a wide dynamic response range for a thick-film ceramic humidity sensor fabricated by a sophisticated procedure, where a change of four orders of magnitude[5] in capacitance was detected. Theoretical explanation for the sensing characteristics of the thick-film ceramic humidity sensor was found to be very complicated by Qu and Meyer[5] and was not discussed in their paper.

The hysteresis loops in Fig. 5 are caused by the difference in RH during adsorption and desorption for a given amount of water condensed in the pores due to the capillary effect. The capillary effect may be described mathematically by the well-known Kelvin equation.[16] Based on this equation, we know that the wider RH range for the hysteresis loop of Sensor B implies a larger range in pore size distribution in the SiO film. This is consistent with the microscopic observations (see Figs. 4 and 6). One may simply attribute the wider dynamic response range in Sensor B to its larger space which water moisture can fill, since through a comparison between Fig. 4 and Fig. 6 we can easily see that the SiO film in Sensor B is much more porous than that in Sensor A. However, it will be shown later that such a simple explanation cannot account for the observed results.

3.2 *Microstructure of top layer*

The microstructure of the top layer also plays an important role in determining the response characteristics of the sensor to the change of RH, since the top layer is the "gate" which controls the passage of moisture to the dielectric. One of the most difficult tasks in the process of this sensor fabrication is to produce a proper capping layer on top of the sensing SiO film. The capping layer must be compact enough to serve as a common electrode and yet still has enough perforations to allow water molecules to move freely in or out of the sensor. A series of deposition experiments showed that the capping layer should be fabricated so that a gold layer with a thickness of a few hundred Å deposited on top of the capping layer can be used as a porous common electrode.

SEM images of the top layers of Sensors A and B are shown in Fig. 7. Analysis of the photos has revealed that the top electrode of Sensor B is more porous than that of Sensor A, and that the pores are more homogeneously distributed in Sensor B than those in Sensor A. The response time of Sensor A is about 75 s, whereas for Sensor B it is less than 3 s. Since water molecules penetrate into the interior of the SiO film mainly through the holes on the surface, the difference in response time between Sensors A and B may at least be partially related to the difference in the microstructures of the top layers. However, since the diameter of water molecules is about 3.87 Å, the surface of Sensor A is presumably porous enough to allow penetration of water molecules. It is plausible, in this particular case, that the slower response time of Sensor A is mainly a result of the helical and relatively compact microstructure of the SiO film, which may create a less permeable barrier to water moisture.

3.3 *Equivalent circuit model*

As shown in Fig. 5, the dynamic response range of Sensor B extends over a surprising five orders of magnitude. To understand this phenomenon, we calculate the largest capacitance that Sensor B can have if the change is caused entirely by the filling of the

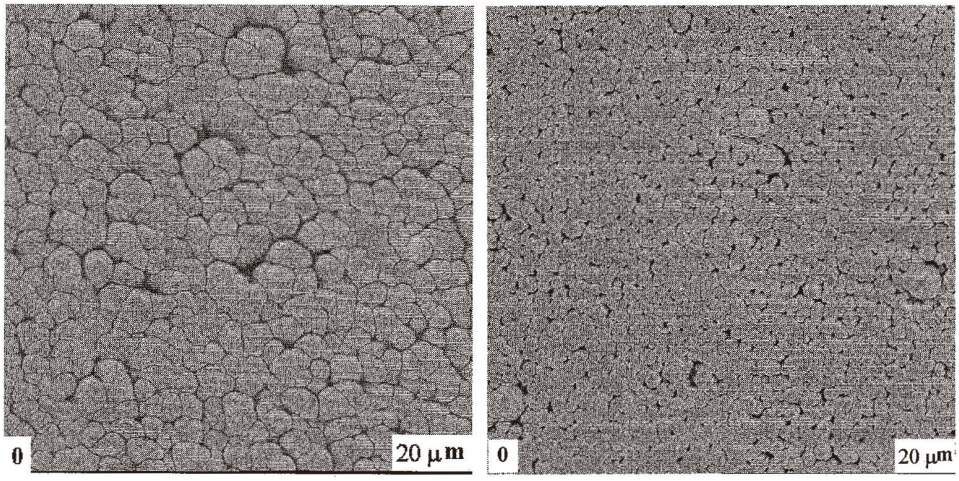

(a) (b)

Fig. 7. SEM top view of (a) Sensor A and (b) Sensor B.

pores by water moisture. Conventionally, the behaviors of RH sensors are understood through the equivalent circuit model. The equivalent circuit of Sensor B may be expressed as shown in Fig. 8, where a detailed equivalent circuit is drawn only for the SiO film. The top capping layer and the bottom more compact SiO film (see Fig. 5) have similar equivalent circuits. Z_t and Z_b in the figure represent the complex impedance of the top capping layer and the bottom compact SiO film, respectively. C_s and R_s are the capacitance and resistance for the SiO film, respectively. Similarly, C_w and R_w are for the pores inside the SiO film, which are presumed to be filled completely by liquid water at high humidity. It may be shown that the total parallel capacitance (C_p) of the system is expressed as

$$C_p = C/2\omega(R^2 + C^2), \tag{1}$$

where ω is the angular frequency of the ac current. R and C are defined as:

$$R = \frac{(R_s + R_w)R_s R_w}{(R_s + R_w)^2 + \omega^2 R_s^2 R_w^2 (C_s + C_w)^2} + \mathrm{Re}(Z_t + Z_b)$$

$$C = \frac{\omega(C_s + C_w)R_s^2 R_w^2}{(R_s + R_w)^2 + \omega^2 R_s^2 R_w^2 (C_s + C_w)^2} - \mathrm{Im}(Z_t + Z_b). \tag{2}$$

Using a computer, the apparent porosity of the SiO film of Sensor B is estimated to be 25% from the top views of SEM images. The porosities of the top capping layer and the bottom

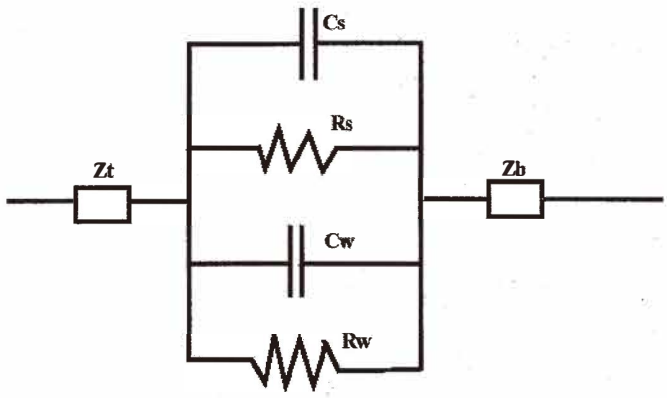

Fig. 8. The equivalent circuit of Sensor B (see text for details).

compact SiO film are taken to be 15%. The dielectric constants of SiO film[17] and liquid water[18] are 5.8 and 78.54 respectively. By taking the resistivities of SiO film[19] and liquid water[15] to be 1.11×10^{7} Ωm and 1.22×10^{4} Ωm, respectively, and using the geometry shown in Fig. 6, the total parallel capacitance is calculated to be 433 pf. This is significantly smaller than the measured value at 97% RH, which is 425 nf (Fig. 5). Note here that in calculating C_p, we take only the pore fraction of the SiO film that contributes to the change in capacitance into account. Those possible pores, voids, or vacancies which are embedded inside the SiO film are not filled with liquid water or water moisture at high RH and are therefore neglected.

To check whether the equivalent circuit model is reasonable, we also calculate the parallel capacitance under dry conditions using the same formulae, assuming R_w is infinite and the dielectric constant of the pores is 1. The result is 75.0 pf. This is remarkably close to the 63 pf measured at 1.1% RH (Fig. 5). The small discrepancy may be a result of the fact that in calculating C_s, we chose the largest possible dielectric constant[17] of 5.8 for the SiO film. Another source of the small discrepancy is a possible uncertainty in determining the apparent porosity of the SiO film.

One may wonder whether the discrepancy in C_p between measured and calculated values at high humidity is a result of the possible small uncertainty in determining the apparent porosity of the SiO film. This is highly unlikely since the calculated C_p under dry conditions agrees with the measured value quite well, implying therefore, that the apparent porosity of SiO estimated from SEM top-view images is reasonable. As an extreme example, one might assume the apparent porosity of the SiO film to be 80% which is the maximum porosity achievable with the GLAD technique. If it is assumed that the pores inside the SiO film are filled completely by liquid water at high humidity, the calculated total parallel capacitance becomes 812 pf. Again this is significantly smaller than the measured value of 425 nf.

This simple model calculation, therefore, suggests that the capacitive response to RH is determined by phenomena other than the simple filling of pores by moisture or liquid water. After RH reaches a certain level, one cannot treat the system as if it were a simple mixture of independent water moisture (or liquid water) and SiO film. It is necessary to take the detailed microstructure of the entire sensor and the interactions between SiO film, water moisture, and the applied field into consideration in calculating C_p. On the other hand, at low RH, the interactions are weak in the present case and can be neglected.

3.4 *Possible explanations*

Since the sensors fabricated here are new in terms of the sensing material, the fabrication technique, and the microstructures of the sensors, it is difficult to apply any existing sensing theories directly to the present case without major modifications, in order to explain the observed sensing characteristics. Development of a new sensing model may be required, particularly for explaining the observed wide dynamic response range of our sensors and for finding a way to minimize or eliminate the undesirable large hysteresis loops shown in Fig. 5. Any appropriate model should consider at least the following three effects on the sensing characteristics of the capacitive SiO RH sensors: a) the effect of capillary condensation of water moisture inside the pores of the sensor, b) the effect of the detailed microstructure of the entire sensor, and c) the effect of the interactions between SiO film, water moisture, and the applied field.

To confirm that the increase of the capacitance in our sensors is due to the admission of the water moisture into the pores of the SiO films, we have carried out measurements on a sample made of a compact SiO film. A change in capacitance from 104 to 156 pf was observed when RH was varied from 0.6% to 98.2%. This change is negligible when compared with those of Sensors A and B (Fig. 5). It is also clear that little, if any, chemical reaction takes place between water and SiO. We immersed a sensor into water for one min, then removed it. One and a half hours later, the measured capacitance was only about 5% larger than that before the immersion.

To explain our observations, first we must investigate the nature of the hygroscopic behavior of SiO films. The hygroscopic property of a material is normally described by the adsorption isotherm. Various adsorption isotherms, resulting from physical adsorption, may be classified into five types according to the BET classification.[20,21] For porous materials, there exist only three types of adsorption isotherms, namely types one, four, and five. These three types can describe the adsorption isotherms of pores of different sizes. Type one is for micropores and types four and five are for intermediate or macropores according to the classification of pores by Dubinin,[22] although there are no sharp borderlines between the classes. From Figs. 4 and 6, we can see that the pore size in Sensor A is much different from that in Sensor B. Therefore, the adsorption isotherm of Sensor A is expected to be significantly different from that of Sensor B. This is one of the major factors contributing to the observed differences in C-RH curves between Sensors A and B.

When porous media are placed in contact with water moisture, several processes occur. With the increase of RH, water molecules may adsorb on the surfaces of the pores, forming a monolayer, then multilayers, and eventually liquid water. The total number of water molecules retained by a porous medium in the first three processes depends on the specific

area of the medium. Different porosities and microstructures in different porous media give different specific areas.

Since both water and SiO are dipolar in nature, the dipole-dipole interaction and the interaction with the applied field cannot be neglected when RH reaches a certain level. Moreover, the strength of the interactions changes with a change in the stage of adsorption. For instance, the interaction at the stage of monolayer coverage of the surfaces of the pores is much different from that when liquid water is formed. These and other factors may result in a remarkable effect on the physical properties at and close to the interface between water and the SiO film, leading to an enhanced dielectric constant for the system. A recently reported and unexplained large capacitance in porous electrochemical capacitors[23] may be based on similar effects. Since the described effects are all microstructure-sensitive, detailed microstructure-related parameters should be included in calculating C_p. Further study regarding the detailed mechanism is under way.

4. Conclusions

We have used relative humidity (RH) sensing as an example to demonstrate the potential of a newly developed film deposition technique called glancing angle deposition (GLAD) in sensing applications. Novel capacitive SiO RH sensors have been fabricated using the GLAD technique which allows the microstructures of deposited films to be controlled in three dimensions on the 10 nm scale. It is shown that the sensing characteristics of the SiO sensors depend critically on the microstructures of the SiO films and their capping layers. By tailoring the microstructures of the SiO films and their capping layers, it is possible to optimize the performance of the sensors if the sensing mechanism is well understood.

At present, it is not completely clear whether humidity sensors based on porous dielectrics fabricated by GLAD have significant advantages over other commonly used capacitive RH sensors. However, our results suggest that the versatility of the GLAD process in engineering the film structure and porosity warrants evaluation of these films in other sensor structures and applications.

Acknowledgments

The authors thank the Natural Sciences and Engineering Research Council of Canada and the Alberta Microelectronic Corporation for financial support, and G. Braybrook for the SEM images.

References

1 K. Carr-Brion: Moisture Sensors in Process Control (Elsevier Appl. Sci. Publishers, London and New York, 1986) Chap. 2.
2 T. Kuroiwa, T. Miyagishi, A. Ito, M. Matsuguchi, Y. Sadaoka and Y. Sakai: Sensors and Actuators B **24–25** (1995) 692.

3 Product specifications of Philips humidity sensor (Model 2322 691 90001) (1999).
4 S. Takeda: Vacuum **41** (1990) 1769.
5 W. Qu and J.-U. Meyer: Sensors and Actuators B **40** (1997) 175.
6 S. Hasegawa: Proc. 30th Electron Components Conference (IEEE, San Francisco, 1980) p. 386.
7 M. Brownawell: Sensors April (1995) 38.
8 K. Robbie and M. J. Brett: J. Vac. Sci. Technol. A **15** (1997) 1460, United States Patent 5866204.
9 K. Robbie, M. J. Brett and A. Lakhtakia: Nature **384** (1996) 616.
10 K. Robbie, A. J. P. Hnatiw, M. J. Brett, R. I. MacDonald and J. N. McMullin: Electronics Lett. **33** (1997) 1213.
11 A. Lakhtakia, R. Messier, M. J. Brett and K. Robbie: Innovations Mater. Res. **1** (1996) 165.
12 J. C. Sit, D. Vick, K. Robbie and M. J. Brett: J. Mater. Res. **14** (1999) 1197.
13 D. Vick, Y. Y. Tsui, M. J. Brett and R. Fedosejevs: Thin Solid Films (in press).
14 Y. Shimizu, H. Ichinose, H. Arai and T. Seiyama: Nippon Kagaku Kaishi (1985) 1270.
15 Y. Shimizu, H. Arai and T. Seiyama: Sensors and Actuators **7** (1985) 11.
16 L. H. Cohan: J. Amer. Chem. Soc. **60** (1938) 433.
17 Handbook of Tables for Applied Engineering Science, ed. R. E. Bolz and G. L. Tuve (The Chemical Rubber Co., Ohio, 1970) p. 210.
18 Handbook of Tables for Applied Engineering Science, ed. R. E. Bolz and G. L. Tuve (The Chemical Rubber Co., Ohio, 1970) p. 68.
19 F. Argall and A. K. Jonscher: Thin Solid Films **2** (1968) 185.
20 S. Brunauer, P. H. Emmett and E. Teller: J. Amer. Chem. Soc. **60** (1938) 309.
21 S. Brunauer, L. S. Deming, W. S. Deming and E. Teller: J. Amer. Chem. Soc. **62** (1940) 1723.
22 M. M. Dubinin: Chem. Rev. **60** (1960) 235.
23 C. Z. Deng, R. A. Pynenburg and K. C. Tsai: J. Electrochem. Soc. **145** (1998) L61.